Random Matrices
MSRI Publications
Volume **65**, 2014

Applications of random matrix theory for sensor array imaging with measurement noise

JOSSELIN GARNIER AND KNUT SØLNA

The imaging of a small target embedded in a medium is a central problem in sensor array imaging. The goal is to find a target embedded in a medium. The medium is probed by an array of sources, and the signals backscattered by the target are recorded by an array of receivers. The responses between all pairs of source and receiver are collected so that the available information takes the form of a response matrix. When the data are corrupted by additive measurement noise we show how tools of random matrix theory can help to detect, localize, and characterize the target.

1. Introduction

The imaging of a small target embedded in a medium is a central problem in wave sensor imaging [Angelsen 2000; Stergiopoulos 2001]. Sensor array imaging involves two steps. The first step is experimental, it consists in emitting waves from an array of sources and recording the backscattered signals by an array of receivers. The data set then consists of a matrix of recorded signals whose indices are the index of the source and the index of the receiver. The second step is numerical, it consists in processing the recorded data in order to estimate the quantities of interest in the medium, such as reflector locations. The main applications of sensor array imaging are medical imaging, geophysical exploration, and nondestructive testing.

Recently it has been shown that random matrix theory could be used in order to build a detection test based on the statistical properties of the singular values of the response matrix [Aubry and Derode 2009a; 2009b; 2010; Ammari et al. 2011; 2012]. This paper summarizes the results contained in [Ammari et al. 2011; 2012] and extends them into several important directions. First we address in this paper the case in which the source array and the receiver array are not coincident, and more generally the case in which the number of sources is different from the number of receivers. As a result the noise singular value distribution has the form of a deformed quarter circle and the statistics of the singular value

MSC2010: primary 78A46; secondary 15B52.

associated to the target is also affected. Second we study carefully the estimation of the noise variance of the response matrix. Different estimators are studied and an estimator that achieves an efficient trade-off between bias and variance is proposed. The use of this estimator instead of the empirical estimator used in the previous versions significantly improves the quality of the detection test based on the singular value distribution of the measured response matrix when the number of sensors is not very large. Third we propose an algorithm that can reconstruct not only the position of the target, but also its scattering amplitude. The estimator of the scattering amplitude compensates for the level repulsion of the singular value associated to the target due to the noise.

2. The response matrix

We address the case of a point reflector that can model a small dielectric anomaly in electromagnetism, a small density anomaly in acoustics, or more generally a local variation of the index of refraction in the scalar wave equation. We consider the case in which the contrast of the anomaly (its index of refraction relative to the one of the background medium) can be of order one but its diameter is assumed to be small compared to the wavelength. In such a situation it is possible to expand the solution of the wave equation around the background solution, as we explain below [Ammari and Kang 2004; Ammari et al. 2001; Ammari and Volkov 2005].

Let us consider the scalar wave equation in a d-dimensional homogeneous medium with the index of refraction n_0. The reference speed of propagation is denoted by c. We assume that the target is a small reflector or inclusion D with the index of refraction $n_{\rm ref} \neq n_0$. The support of the inclusion is of the form $D = \boldsymbol{x}_{\rm ref} + B$, where B is a domain with small volume and $\boldsymbol{x}_{\rm ref}$ is the location of the reflector. Therefore the scalar wave equation with the source $S(t, \boldsymbol{x})$ takes the form

$$\frac{n^2(\boldsymbol{x})}{c^2}\partial_t^2 E - \Delta_{\boldsymbol{x}} E = S(t, \boldsymbol{x}),$$

where the index of refraction is given by

$$n(\boldsymbol{x}) = n_0 + (n_{\rm ref} - n_0)\mathbf{1}_D(\boldsymbol{x}).$$

In this paper we consider time-harmonic point sources emitting at frequency ω. For any $\boldsymbol{y}_n, \boldsymbol{z}_m$ far from $\boldsymbol{x}_{\rm ref}$ the field $\mathrm{Re}(\hat{E}(\boldsymbol{y}_n, \boldsymbol{z}_m)e^{-i\omega t})$ observed at $\boldsymbol{y}_n$ when a point source emits a time-harmonic signal with frequency ω at $\boldsymbol{z}_m$ can be expanded as powers of the volume of the inclusion as

$$\hat{E}(\boldsymbol{y}_n, \boldsymbol{z}_m) = \hat{G}(\boldsymbol{y}_n, \boldsymbol{z}_m) + k_0^2 \rho_{\rm ref} \hat{G}(\boldsymbol{y}_n, \boldsymbol{x}_{\rm ref})\hat{G}(\boldsymbol{x}_{\rm ref}, \boldsymbol{z}_m) + O\big(|B|^{\frac{d+1}{d}}\big), \quad (1)$$

where $k_0 = n_0\omega/c$ is the homogeneous wavenumber, ρ_{ref} is the scattering amplitude

$$\rho_{\text{ref}} = \left(\frac{n_{\text{ref}}^2}{n_0^2} - 1\right)|B|, \tag{2}$$

and $\hat{G}(\boldsymbol{x}, \boldsymbol{z})$ is the Green's function or fundamental solution of the Helmholtz equation with a point source at $\boldsymbol{z}$:

$$\Delta_{\boldsymbol{x}}\hat{G}(\boldsymbol{x}, \boldsymbol{z}) + k_0^2\hat{G}(\boldsymbol{x}, \boldsymbol{z}) = -\delta(\boldsymbol{x} - \boldsymbol{z}). \tag{3}$$

More explicitly we have

$$\hat{G}(\boldsymbol{x}, \boldsymbol{z}) = \begin{cases} \dfrac{i}{4}H_0^{(1)}(k_0|\boldsymbol{x} - \boldsymbol{z}|) & \text{if } d = 2, \\ \dfrac{e^{ik_0|\boldsymbol{x}-\boldsymbol{z}|}}{4\pi|\boldsymbol{x} - \boldsymbol{z}|} & \text{if } d = 3, \end{cases}$$

where $H_0^{(1)}$ is the Hankel function of the first kind of order zero.

When there are M sources $(\boldsymbol{z}_m)_{m=1,\ldots,M}$ and N receivers $(\boldsymbol{y}_n)_{n=1,\ldots,N}$, the response matrix is the $N \times M$ matrix $\boldsymbol{A}_0 = (A_{0,nm})_{n=1,\ldots,N,m=1,\ldots,M}$ defined by

$$A_{0,nm} := \hat{E}(\boldsymbol{y}_n, \boldsymbol{z}_m) - \hat{G}(\boldsymbol{y}_n, \boldsymbol{z}_m). \tag{4}$$

This matrix has rank one:

$$\boldsymbol{A}_0 = \sigma_{\text{ref}}\boldsymbol{u}_{\text{ref}}\boldsymbol{v}_{\text{ref}}^{\dagger}, \tag{5}$$

where $\dagger$ stands for the conjugate transpose. The unique nonzero singular value of this matrix is

$$\sigma_{\text{ref}} = k_0^2\rho_{\text{ref}}\left(\sum_{l=1}^{N}|\hat{G}(\boldsymbol{y}_l, \boldsymbol{x}_{\text{ref}})|^2\right)^{1/2}\left(\sum_{l=1}^{M}|\hat{G}(\boldsymbol{z}_l, \boldsymbol{x}_{\text{ref}})|^2\right)^{1/2}. \tag{6}$$

The associated left and right singular vectors $\boldsymbol{u}_{\text{ref}}$ and $\boldsymbol{v}_{\text{ref}}$ are given by

$$\boldsymbol{u}_{\text{ref}} = \boldsymbol{u}(\boldsymbol{x}_{\text{ref}}), \qquad \boldsymbol{v}_{\text{ref}} = \boldsymbol{v}(\boldsymbol{x}_{\text{ref}}), \tag{7}$$

where we have defined the normalized vectors of Green's functions:

$$\begin{aligned} \boldsymbol{u}(\boldsymbol{x}) &= \left(\frac{\hat{G}(\boldsymbol{y}_n, \boldsymbol{x})}{\left(\sum_{l=1}^{N}|\hat{G}(\boldsymbol{y}_l, \boldsymbol{x})|^2\right)^{1/2}}\right)_{n=1,\ldots,N}, \\ \boldsymbol{v}(\boldsymbol{x}) &= \left(\frac{\overline{\hat{G}(\boldsymbol{z}_m, \boldsymbol{x})}}{\left(\sum_{l=1}^{M}|\hat{G}(\boldsymbol{z}_l, \boldsymbol{x})|^2\right)^{1/2}}\right)_{m=1,\ldots,M}. \end{aligned} \tag{8}$$

The matrix $\boldsymbol{A}_0$ is the complete data set that can be collected. In practice the measured matrix is corrupted by electronic or measurement noise that has the form of an additive noise, with uncorrelated entries. The purpose of this paper is to address the classical imaging problems given the measured data set:

(1) Is there a target in the medium? This is the detection problem. In the absence of noise this question is trivial in that we can claim that there is a target buried in the medium as soon as the response matrix is not zero. In the presence of noise, it is not so obvious to answer this question since the response matrix is not zero due to additive noise even in the absence of a target. Our purpose is to build a detection test that has the maximal probability of detection for a given false alarm rate.

(2) Where is the target? This is the localization problem. Several methods can be proposed, essentially based on the back-propagation of the data set, and we will describe robust methods in the presence of noise.

(3) What are the characteristic properties of the target? This is the reconstruction problem. One may look after geometric and physical properties. In fact, in view of the expression (1)–(2), only the product of the volume of the inclusion times the contrast can be identified in the regime we address in this paper.

The paper is organized as follows. In Section 3 we explain how the data should be collected to minimize the impact of the additive noise. In Section 4 we give results about the distribution of the singular values of the response matrix, with special attention on the maximal singular value. In Section 5 we discuss how the noise level can be estimated with minimal bias and variance. In Section 6 we build a test for the detection of the target and in Section 7 we show how the position and the scattering amplitude of the target can be estimated.

3. Data acquisition

In this section we consider that there are M sources and N receivers. The measures are noisy, which means that the signal measured by a receiver is corrupted by an additive noise that can be described in terms of a circular complex Gaussian random variable with mean zero and variance σ_{n}^2. The recorded noises are independent from each other.

In the standard acquisition scheme, the response matrix is measured during a sequence of M experiments. In the m-th experience, $m = 1, \ldots, M$, the m-th source (located at $\boldsymbol{z}_m$) generates a time-harmonic signal with unit amplitude and the N receivers (located at $\boldsymbol{y}_n$, $n = 1, \ldots, N$) record the backscattered waves

which means that they measure

$$A_{\text{meas},nm} = A_{0,nm} + W_{nm}, \quad n = 1, \ldots, N, \quad m = 1, \ldots, M,$$

which gives the matrix

$$\boldsymbol{A}_{\text{meas}} = \boldsymbol{A}_0 + \boldsymbol{W}, \tag{9}$$

where $\boldsymbol{A}_0$ is the unperturbed response matrix of rank one (4) and W_{nm} are independent complex Gaussian random variables with mean zero and variance σ_{n}^2.

The Hadamard technique is a noise reduction technique in the presence of additive noise that uses the structure of Hadamard matrices.

Definition 3.1. A complex Hadamard matrix $\boldsymbol{H}$ of order M is a $M \times M$ matrix whose elements are of modulus one and such that $\boldsymbol{H}^\dagger \boldsymbol{H} = M\boldsymbol{I}$.

Complex Hadamard matrices exist for all M. For instance the Fourier matrix

$$H_{nm} = \exp\left[i2\pi \frac{(n-1)(m-1)}{M}\right], \quad m, n = 1, \ldots, M, \tag{10}$$

is a complex Hadamard matrix. A Hadamard matrix has maximal determinant among matrices with complex entries in the closed unit disk. More exactly Hadamard [1893] proved that the determinant of any complex $M \times M$ matrix $\boldsymbol{H}$ with entries in the closed unit disk satisfies $|\det \boldsymbol{H}| \leq M^{M/2}$, with equality attained by a complex Hadamard matrix.

We now describe a general multisource acquisition scheme and show the importance of Hadamard matrices to build an optimal scheme. Let $\boldsymbol{H}$ be an invertible $M \times M$ matrix with complex entries in the closed unit disk. In the multisource acquisition scheme, the response matrix is measured during a sequence of M experiments. In the m-th experience, $m = 1, \ldots, M$, all sources generate time-harmonic signals with unit amplitude or smaller, the m' source generating $H_{m'm}$ for $m' = 1, \ldots, M$. In other words, in the m-th experiment, we can use all the sources up to their maximal transmission power (which we have normalized to one) and we are free to choose their phases in order to minimize the effective noise level in the recorded data. In the m-th experiment, the N receivers record the backscattered waves, which means that they measure

$$B_{\text{meas},nm} = \sum_{m'=1}^{M} H_{m'm} A_{0,nm'} + W_{nm} = (\boldsymbol{A}_0 \boldsymbol{H})_{nm} + W_{nm}, \quad n = 1, \ldots, N.$$

Collecting the recorded signals of the M experiments gives the matrix

$$\boldsymbol{B}_{\text{meas}} = \boldsymbol{A}_0 \boldsymbol{H} + \boldsymbol{W},$$

where $\boldsymbol{A}_0$ is the unperturbed response matrix and W_{nm} are independent complex Gaussian random variables with mean zero and variance $\sigma_{\rm n}^2$. The measured response matrix $\boldsymbol{A}_{\rm meas}$ is obtained by right multiplying the matrix $\boldsymbol{B}_{\rm meas}$ by the matrix $\boldsymbol{H}^{-1}$:

$$\boldsymbol{A}_{\rm meas} := \boldsymbol{B}_{\rm meas}\boldsymbol{H}^{-1} = \boldsymbol{A}_0\boldsymbol{H}\boldsymbol{H}^{-1} + \boldsymbol{W}\boldsymbol{H}^{-1}, \tag{11}$$

so that we get the unperturbed matrix $\boldsymbol{A}_0$ up to a new noise

$$\boldsymbol{A}_{\rm meas} = \boldsymbol{A}_0 + \widetilde{\boldsymbol{W}}, \qquad \widetilde{\boldsymbol{W}} = \boldsymbol{W}\boldsymbol{H}^{-1}. \tag{12}$$

The choice of the matrix $\boldsymbol{H}$ should fulfill the property that the new noise matrix $\widetilde{\boldsymbol{W}}$ has independent complex entries with Gaussian statistics, mean zero, and minimal variance. We have

$$\begin{aligned}\mathbb{E}\big[\overline{\widetilde{W}_{nm}}\widetilde{W}_{n'm'}\big] &= \sum_{q,q'=1}^{M} \overline{(\boldsymbol{H}^{-1})_{q m}}(\boldsymbol{H}^{-1})_{q'm'}\mathbb{E}\big[\overline{W_{nq}}W_{n'q'}\big] \\ &= \sigma_{\rm n}^2((\boldsymbol{H}^{-1})^{\dagger}\boldsymbol{H}^{-1})_{mm'}\mathbf{1}_n(n').\end{aligned}$$

This shows that we look for a complex matrix $\boldsymbol{H}$ with entries in the unit disk such that $(\boldsymbol{H}^{-1})^{\dagger}\boldsymbol{H}^{-1} = c\boldsymbol{I}$ with a minimal c. This is equivalent to require that $\boldsymbol{H}$ is unitary and that $|\det \boldsymbol{H}|$ is maximal. Using Hadamard result we know that the maximal determinant is $M^{M/2}$ and that a complex Hadamard matrix attains the maximum. Therefore a matrix $\boldsymbol{H}$ that minimizes the noise variance should be a Hadamard matrix, such as, for instance, the Fourier matrix (10). Note that, in the case of a linear array, the use of a Fourier matrix corresponds to an illumination in the form of plane waves with regularly sampled angles.

When the multisource acquisition scheme is used with a Hadamard technique, we have $\boldsymbol{H}^{-1} = \frac{1}{M}\boldsymbol{H}^{\dagger}$ and the new noise matrix $\widetilde{\boldsymbol{W}}$ in (12) has independent complex entries with Gaussian statistics, mean zero, and variance $\sigma_{\rm n}^2/M$:

$$\mathbb{E}\big[\overline{\widetilde{W}_{nm}}\widetilde{W}_{n'm'}\big] = \frac{\sigma_{\rm n}^2}{M}\mathbf{1}_m(m')\mathbf{1}_n(n'). \tag{13}$$

This gain of a factor M in the signal-to-noise ratio is called the Hadamard advantage.

4. Singular value decomposition of the response matrix

Singular values of a noisy matrix. We consider here the situation in which the measured response matrix $\boldsymbol{A}_{\rm meas}$ consists of independent noise coefficients with mean zero and variance $\sigma_{\rm n}^2/M$ and the number of receivers is larger than the number of sources $N \geq M$. As shown in the previous section, this is the case

when the response matrix is acquired with the Hadamard technique and there is no target in the medium.

We denote by $\sigma_1^{(M)} \geq \sigma_2^{(M)} \geq \sigma_3^{(M)} \geq \cdots \geq \sigma_M^{(M)}$ the singular values of the response matrix $\boldsymbol{A}_{\text{meas}}$ sorted by decreasing order and by $\Lambda^{(M)}$ the corresponding integrated density of states defined by

$$\Lambda^{(M)}([\sigma_u, \sigma_v]) := \frac{1}{M}\text{Card}\big\{l = 1, \ldots, M\ ,\ \sigma_l^{(M)} \in [\sigma_u, \sigma_v]\big\} \quad \text{for } \sigma_u < \sigma_v. \tag{14}$$

For large N and M with $N/M = \gamma \geq 1$ fixed we have the following results which are classical in random matrix theory [Marchenko and Pastur 1967; Johnstone 2001; Capitaine et al. 2012].

Proposition 4.1. (a) *The random measure $\Lambda^{(M)}$ almost surely converges to the deterministic absolutely continuous measure Λ with compact support*:

$$\Lambda([\sigma_u, \sigma_v]) = \int_{\sigma_u}^{\sigma_v} \frac{1}{\sigma_{\text{n}}}\rho_\gamma\left(\frac{\sigma}{\sigma_{\text{n}}}\right)d\sigma, \quad 0 \leq \sigma_u \leq \sigma_v, \tag{15}$$

where ρ_γ is the deformed quarter-circle law given by

$$\rho_\gamma(x) = \begin{cases} \dfrac{1}{\pi x}\sqrt{\big((\gamma^{\frac{1}{2}}+1)^2 - x^2\big)\big(x^2 - (\gamma^{\frac{1}{2}}-1)^2\big)} & \text{if } \gamma^{\frac{1}{2}}-1 < x \leq \gamma^{\frac{1}{2}}+1, \\ 0 & \text{otherwise}. \end{cases} \tag{16}$$

(b) *The normalized l^2-norm of the singular values satisfies*

$$M\left[\frac{1}{M}\sum_{j=1}^{M}(\sigma_j^{(M)})^2 - \gamma\sigma_{\text{n}}^2\right] \overset{M\to\infty}{\longrightarrow} \sqrt{\gamma}\sigma_{\text{n}}^2 Z_0 \quad \text{in distribution}, \tag{17}$$

where Z_0 follows a Gaussian distribution with mean zero and variance one.

(c) *The maximal singular value satisfies*

$$M^{\frac{2}{3}}\big[\sigma_1^{(M)} - \sigma_{\text{n}}(\gamma^{\frac{1}{2}}+1)\big] \overset{M\to\infty}{\longrightarrow} \frac{\sigma_{\text{n}}}{2}(1+\gamma^{-\frac{1}{2}})^{\frac{1}{3}} Z_2 \quad \text{in distribution}, \tag{18}$$

where Z_2 follows a type-2 Tracy–Widom distribution.

The type-2 Tracy–Widom distribution has the cumulative distribution function Φ_{TW2} given by

$$\Phi_{\text{TW2}}(z) = \exp\left(-\int_z^\infty (x-z)\varphi^2(x)\,dx\right), \tag{19}$$

where $\varphi(x)$ is the solution of the Painlevé equation

$$\varphi''(x) = x\varphi(x) + 2\varphi(x)^3, \quad \varphi(x) \simeq \text{Ai}(x),\ x \to \infty, \tag{20}$$

Ai being the Airy function. The expectation and variance of Z_2 are

$$\mathbb{E}[Z_2] \simeq -1.77 \quad \text{and} \quad \mathrm{Var}(Z_2) \simeq 0.81.$$

Detailed results about the Tracy–Widom distributions can be found in [Baik et al. 2008] and their numerical evaluations are addressed in [Bornemann 2010].

Singular values of the perturbed response matrix. The measured response matrix using the Hadamard technique in the presence of a target and in the presence of measurement noise is

$$\boldsymbol{A}_{\mathrm{meas}} = \boldsymbol{A}_0 + \boldsymbol{W}, \tag{21}$$

where $\boldsymbol{A}_0$ is given by (4) and $\boldsymbol{W}$ has independent random complex entries with Gaussian statistics, mean zero and variance σ_{n}^2/M. We consider the critical and interesting regime in which the singular values of the unperturbed matrix are of the same order as the singular values of the noise, that is to say, σ_{ref} is of the same order of magnitude as σ_{n}. The following proposition shows that there is a phase transition:

(1) Either the noise level σ_{n} is smaller than the critical value $\gamma^{-1/4}\sigma_{\mathrm{ref}}$ and then the maximal singular value of the perturbed response matrix is a perturbation of the nonzero singular value of the unperturbed response matrix; this perturbation has Gaussian statistics with a mean of order one and a variance of the order of $1/M$.

(2) Or the noise level σ_{n} is larger than the critical value $\gamma^{-1/4}\sigma_{\mathrm{ref}}$ and then the nonzero singular value of the unperturbed response matrix is buried in the deformed quarter circle distribution of the pure noise matrix and the maximal singular value of the perturbed response matrix has a behavior similar to the pure noise case (described in Proposition 4.1).

Proposition 4.2. *In the regime $M \to \infty$:*

(a) *The normalized l^2-norm of the singular values satisfies*

$$M\left[\frac{1}{M}\sum_{j=1}^{M}(\sigma_j^{(M)})^2 - \gamma\sigma_{\mathrm{n}}^2\right] \overset{M\to\infty}{\longrightarrow} \sigma_{\mathrm{ref}}^2 + \sqrt{2\gamma}\sigma_{\mathrm{n}}^2 Z_0 \quad \textit{in distribution}, \tag{22}$$

where Z_0 follows a Gaussian distribution with mean zero and variance one.

(b1) *If $\sigma_{\mathrm{ref}} < \gamma^{1/4}\sigma_{\mathrm{n}}$, the maximal singular value satisfies*

$$\sigma_1^{(M)} \overset{M\to\infty}{\longrightarrow} \sigma_{\mathrm{n}}(\gamma^{\frac{1}{2}} + 1) \quad \textit{in probability}. \tag{23}$$

More exactly,

$$M^{\frac{2}{3}}\left[\sigma_1^{(M)} - \sigma_{\mathrm{n}}\left(\gamma^{\frac{1}{2}}+1\right)\right] \overset{M\to\infty}{\longrightarrow} \tfrac{1}{2}\sigma_{\mathrm{n}}\left(1+\gamma^{-\frac{1}{2}}\right)^{\frac{1}{3}} Z_2 \quad \textit{in distribution}, \tag{24}$$

where Z_2 follows a type-2 Tracy–Widom distribution.

(b2) *If $\sigma_{\mathrm{ref}} > \gamma^{1/4}\sigma_{\mathrm{n}}$, then the maximal singular value satisfies*

$$\sigma_1^{(M)} \overset{M\to\infty}{\longrightarrow} \sigma_{\mathrm{ref}}\left(1+\gamma\frac{\sigma_{\mathrm{n}}^2}{\sigma_{\mathrm{ref}}^2}\right)^{\frac{1}{2}}\left(1+\frac{\sigma_{\mathrm{n}}^2}{\sigma_{\mathrm{ref}}^2}\right)^{\frac{1}{2}} \quad \textit{in probability}. \tag{25}$$

More exactly,

$$M^{\frac{1}{2}}\left[\sigma_1^{(M)} - \sigma_{\mathrm{ref}}\left(1+\gamma\frac{\sigma_{\mathrm{n}}^2}{\sigma_{\mathrm{ref}}^2}\right)^{\frac{1}{2}}\left(1+\frac{\sigma_{\mathrm{n}}^2}{\sigma_{\mathrm{ref}}^2}\right)^{\frac{1}{2}}\right] \overset{M\to\infty}{\longrightarrow} \frac{\sigma_{\mathrm{n}}}{2}\frac{\left(1-\gamma\sigma_{\mathrm{n}}^4/\sigma_{\mathrm{ref}}^4\right)^{\frac{1}{2}}\left(2+(1+\gamma)\sigma_{\mathrm{n}}^2/\sigma_{\mathrm{ref}}^2\right)^{\frac{1}{2}}}{\left(1+\gamma\sigma_{\mathrm{n}}^2/\sigma_{\mathrm{ref}}^2\right)^{\frac{1}{2}}\left(1+\sigma_{\mathrm{n}}^2/\sigma_{\mathrm{ref}}^2\right)^{\frac{1}{2}}} Z_0, \tag{26}$$

in distribution, where Z_0 follows a Gaussian distribution with mean zero and variance one.

These results are illustrated in Figure 1. Their proofs can be obtained from the method described in [Benaych-Georges and Nadakuditi 2011]. Extensions to heteroscedastic noise can also be obtained as in [Chapon et al. 2014]. Note that formula (26) seems to predict that the standard deviation of the maximal singular value cancels when $\sigma_{\mathrm{ref}} \searrow \gamma^{1/4}\sigma_{\mathrm{n}}$, but this is true only to the order $M^{-1/2}$, and in fact it becomes of order $M^{-2/3}$ (see Figure 1). Following [Baik et al. 2005] we can anticipate that there are interpolating distributions which appear when

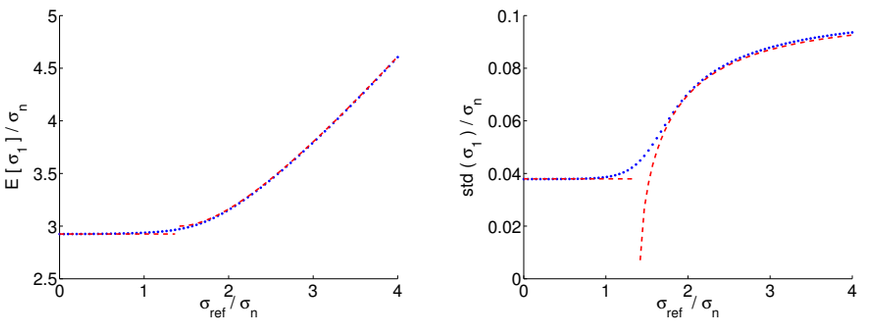

Figure 1. Mean and standard deviation of the maximal singular value. We compare the empirical means (left) and standard deviations (right) obtained from 10^4 MC simulations (blue dots) with the theoretical formulas given in Proposition 4.2 (red dashed lines). Here $N = 200$ and $M = 50$ ($\gamma = 4$).

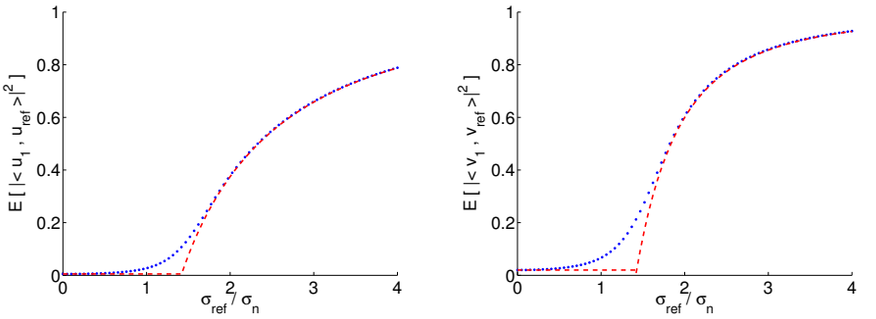

Figure 2. Means of the square angles between the perturbed and unperturbed singular vectors. We compare the empirical means obtained from 10^4 MC simulations (blue dots) with the theoretical formulas given in Proposition 4.3 (red dashed lines). Here $N = 200$ and $M = 50$ ($\gamma = 4$).

$\sigma_{\rm ref} = \gamma^{1/4}\sigma_{\rm n} + wM^{-1/3}$ for some fixed w. This problem deserves a detailed study.

Singular vectors of the perturbed response matrix. It is of interest to describe the statistical distribution of the angle between the left singular vector $\boldsymbol{u}_1^{(M)}$ (resp. right singular vector $\boldsymbol{v}_1^{(M)}$) of the noisy matrix $\boldsymbol{A}_{\rm meas}$ and the left singular vector $\boldsymbol{u}(\boldsymbol{x}_{\rm ref})$ (resp. right singular vector $\boldsymbol{v}(\boldsymbol{x}_{\rm ref})$) of the unperturbed matrix $\boldsymbol{A}_0$. This justifies the MUSIC-based algorithm for the target localization algorithm that we discuss in Section 7.

Proposition 4.3. *We consider the case* $\sigma_{\rm ref} > \gamma^{\frac{1}{4}}\sigma_{\rm n}$. *When* $\gamma = N/M$ *is fixed and* $M \to \infty$, *we have in probability*

$$\begin{aligned} \left|(\boldsymbol{u}_1^{(M)})^\dagger \boldsymbol{u}(\boldsymbol{x}_{\rm ref})\right|^2 &\stackrel{M\to\infty}{\longrightarrow} \frac{1-\gamma\sigma_{\rm n}^4/\sigma_{\rm ref}^4}{1+\gamma\sigma_{\rm n}^2/\sigma_{\rm ref}^2}, \\ \left|(\boldsymbol{v}_1^{(M)})^\dagger \boldsymbol{v}(\boldsymbol{x}_{\rm ref})\right|^2 &\stackrel{M\to\infty}{\longrightarrow} \frac{1-\gamma\sigma_{\rm n}^4/\sigma_{\rm ref}^4}{1+\sigma_{\rm n}^2/\sigma_{\rm ref}^2}. \end{aligned} \tag{27}$$

Proposition 4.3 shows that the first singular vectors of the perturbed matrix $\boldsymbol{A}_{\rm meas}$ have deterministic angles with respect to the first singular vectors of the unperturbed matrix $\boldsymbol{A}_0$ provided the first singular value emerges from the deformed quarter-circle distribution. These results are proved in [Benaych-Georges and Nadakuditi 2011] and they are illustrated in Figure 2.

5. The evaluation of the noise level

Empirical estimator. The truncated normalized l^2-norm of the singular values satisfies (22). Therefore the truncated normalized l^2-norm of the singular values

satisfies

$$M\left[\frac{1}{M-(1+\gamma^{-\frac{1}{2}})^2}\sum_{j=2}^{M}(\sigma_j^{(M)})^2-\gamma\sigma_{\mathrm{n}}^2\right]\overset{M\to\infty}{\longrightarrow} b_1+\sqrt{\gamma}\sigma_{\mathrm{n}}^2 Z_0 \quad \text{in distribution,}$$

where Z_0 follows a Gaussian distribution with mean zero and variance one, and the asymptotic bias is

$$b_1 = \sigma_{\mathrm{ref}}^2 - \bar{\sigma}_1^2 + \sigma_{\mathrm{n}}^2(1+\gamma^{\frac{1}{2}})^2. \tag{28}$$

Here

$$\bar{\sigma}_1 = \max\left\{\sigma_{\mathrm{ref}}\left(1+\gamma\frac{\sigma_{\mathrm{n}}^2}{\sigma_{\mathrm{ref}}^2}\right)^{\frac{1}{2}}\left(1+\frac{\sigma_{\mathrm{n}}^2}{\sigma_{\mathrm{ref}}^2}\right)^{\frac{1}{2}},\ \sigma_{\mathrm{n}}(1+\gamma^{\frac{1}{2}})\right\} \tag{29}$$

is the deterministic leading-order value of the maximal singular value as shown in Proposition 4.2. The normalization in the truncated l^2-norm has been chosen so that, in the absence of a target, the asymptotic bias is zero: $b_1\,|_{\sigma_{\mathrm{ref}}=0} = 0$. This implies that

$$\hat{\sigma}_{\mathrm{n}}^e := \gamma^{-\frac{1}{2}}\left[\frac{1}{M-(1+\gamma^{-\frac{1}{2}})^2}\sum_{j=2}^{M}\left(\sigma_j^{(M)}\right)^2\right]^{\frac{1}{2}} \tag{30}$$

is an empirical estimator of σ_{n} with Gaussian fluctuations of the order of M^{-1}. This estimator satisfies

$$M[\hat{\sigma}_{\mathrm{n}}^e-\sigma_{\mathrm{n}}]\overset{M\to\infty}{\longrightarrow}\frac{b_1}{2\gamma\sigma_{\mathrm{n}}}+\frac{\sigma_{\mathrm{n}}}{2\gamma^{\frac{1}{2}}}Z_0 \quad \text{in distribution,}$$

and therefore

$$\hat{\sigma}_{\mathrm{n}}^e = \sigma_{\mathrm{n}} + o\left(\frac{1}{M^{\frac{2}{3}}}\right) \quad \text{in probability.} \tag{31}$$

The empirical estimator is easy to compute, since it requires the evaluation of the Frobenius norm of the measured matrix $\boldsymbol{A}_{\mathrm{meas}}$ and the maximal singular value:

$$\hat{\sigma}_{\mathrm{n}}^e = \gamma^{-\frac{1}{2}}\left[\frac{\sum_{n=1}^{N}\sum_{m=1}^{M}|A_{nm}|^2-\left(\sigma_1^{(M)}\right)^2}{M-(1+\gamma^{-\frac{1}{2}})^2}\right]^{\frac{1}{2}}. \tag{32}$$

Corrected empirical estimator. It is possible to improve the quality of the estimation of the noise level and to cancel the bias of the empirical estimator. Using Proposition 4.2 we can see that the quantity

$$\hat{\sigma}_{\mathrm{ref}}^e = \frac{\hat{\sigma}_{\mathrm{n}}^e}{\sqrt{2}}\left\{\left(\frac{\sigma_1^{(M)}}{\hat{\sigma}_{\mathrm{n}}^e}\right)^2-1-\gamma+\left(\left[\left(\frac{\sigma_1^{(M)}}{\hat{\sigma}_{\mathrm{n}}^e}\right)^2-1-\gamma\right]^2-4\gamma\right)^{\frac{1}{2}}\right\}^{\frac{1}{2}} \tag{33}$$

is an estimator of σ_{ref}, provided that $\sigma_{\text{ref}} > \gamma^{1/4}\sigma_{\text{n}}$. Therefore, when $\sigma_{\text{ref}} > \gamma^{1/4}\sigma_{\text{n}}$, it is possible to build an improved estimator of the noise variance by removing from the empirical estimator an estimation of the asymptotic bias which is itself based on the empirical estimator $\hat{\sigma}_{\text{n}}^e$. The estimator of the asymptotic bias that we propose to use is

$$\hat{b}_1^e = (\hat{\sigma}_{\text{ref}}^e)^2 - \left(\sigma_1^{(M)}\right)^2 + (\hat{\sigma}_{\text{n}}^e)^2(1+\gamma^{\frac{1}{2}})^2, \tag{34}$$

and therefore we can propose the following estimator of the noise level σ_{n}:

$$\hat{\sigma}_{\text{n}}^c := \hat{\sigma}_{\text{n}}^e - \frac{\hat{b}_1^e}{2\gamma M \hat{\sigma}_{\text{n}}^e}. \tag{35}$$

This estimator satisfies

$$M[\hat{\sigma}_{\text{n}}^c - \sigma_{\text{n}}] \overset{M\to\infty}{\longrightarrow} \frac{\sigma_{\text{n}}}{2\gamma^{\frac{1}{2}}} Z_0 \quad \text{in distribution.} \tag{36}$$

This estimator can only be used when $\hat{\sigma}_{\text{ref}}^e > \gamma^{1/4}\hat{\sigma}_{\text{n}}^e$ and it should then be preferred to the empirical estimator $\hat{\sigma}_{\text{n}}^e$.

Kolmogorov–Smirnov estimator. An alternative method to estimate σ_{n} is the approach outlined in [Györfi et al. 1996] and applied in [Shabalin and Nobel 2013], which consists in minimizing the Kolmogorov–Smirnov distance $\mathscr{D}(\sigma)$ between the observed sample distribution of the $M-K$ smallest singular values of the measured matrix $\boldsymbol{A}_{\text{meas}}$ and that predicted by theory, which is the deformed quarter circle distribution (16) parametrized by σ_{n}. Compared to [Györfi et al. 1996; Shabalin and Nobel 2013] we here introduce a cut-off parameter K that can be chosen by the user. All choices are equivalent in the asymptotic framework $M \to \infty$, but for finite M low values for K give estimators with small variances but with bias, while large values for K increase the variance but decay the bias (see Figure 3). We define the new estimator $\hat{\sigma}_{\text{n}}^K$ of σ_{n} as the parameter that minimizes the Kolmogorov–Smirnov distance. After elementary manipulations we find that the Kolmogorov–Smirnov estimator is of the form

$$\hat{\sigma}_{\text{n}}^K := \operatorname*{argmin}_{\sigma>0} \mathscr{D}_K^{(M)}(\sigma), \tag{37}$$

where $\mathscr{D}_K^{(M)}(\sigma)$ is defined by

$$\mathscr{D}_K^{(M)}(\sigma) := \max_{m=1,\dots,M-K} \left| G_\gamma\left(\frac{\sigma_{M+1-m}^{(M)}}{\sigma}\right) - \frac{m-1/2}{M} \right| + \frac{1}{2M}, \tag{38}$$

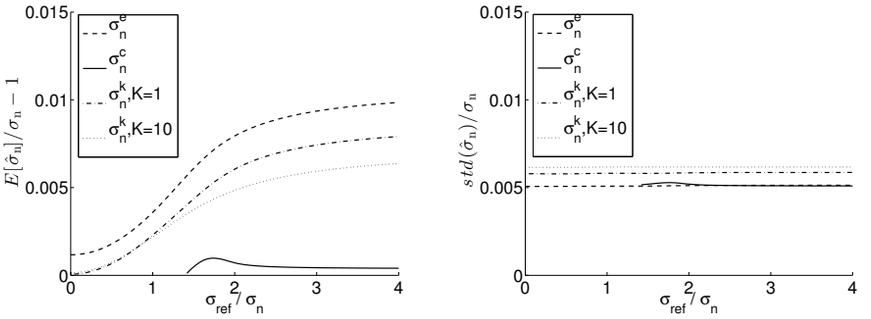

Figure 3. Relative bias (left) and standard deviations (right) of different estimators of the noise level. Here $N = 200$ and $M = 50$ ($\gamma = 4$).

G_γ is the cumulative distribution function with density (16):

$$G_\gamma(x) = \begin{cases} 0 & \text{if } x \le \gamma^{\frac{1}{2}} - 1, \\ \dfrac{1}{2} + \dfrac{\gamma^{\frac{1}{2}}}{\pi}(1 - G(x)^2)^{\frac{1}{2}} - \dfrac{\gamma+1}{\pi} \arcsin G(x) & \\ \quad - \dfrac{\gamma-1}{\pi} \arctan \dfrac{1 - (\gamma^{\frac{1}{2}} + \gamma^{-\frac{1}{2}})G(x)}{(1-G(x)^2)^{\frac{1}{2}}(\gamma^{\frac{1}{2}} - \gamma^{-\frac{1}{2}})} & \text{if } \gamma^{\frac{1}{2}} - 1 < x \le \gamma^{\frac{1}{2}} + 1, \\ 1 & \text{if } \gamma^{\frac{1}{2}} + 1 < x, \end{cases}$$

with

$$G(x) = \frac{(1+\gamma) - x^2}{2\gamma^{\frac{1}{2}}}.$$

If $\gamma = 1$, we have

$$G_1(x) = \begin{cases} 0 & \text{if } x \le 0, \\ \dfrac{1}{2\pi}\left(x\sqrt{4 - x^2} + 4 \arcsin \dfrac{x}{2}\right) & \text{if } 0 < x \le 2, \\ 1 & \text{if } 2 < x. \end{cases}$$

Discussion. The three estimation methods described in the three previous subsections have been implemented and numerical results are reported in Figure 3.

As predicted by the asymptotic theory, the variance of the empirical estimator is equivalent to the one of the corrected empirical estimator, and they are smaller than the ones of the Kolmogorov–Smirnov estimator. The bias of the empirical estimator is larger than the bias of the Kolmogorov–Smirnov estimator. The corrected empirical estimator has a very small bias. The variance of the

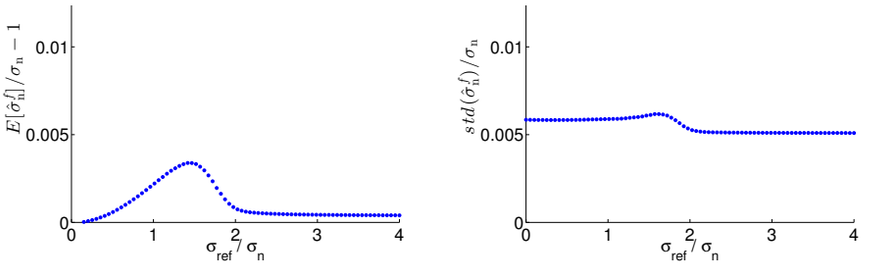

Figure 4. Relative bias (left) and standard deviations (right) of the final estimator (39) of the noise level. Here $N = 200$ and $M = 50$ ($\gamma = 4$).

Kolmogorov–Smirnov estimator increases with K, but its bias decreases with increasing K. From these observations we conclude:

• When $\hat{\sigma}_{\rm ref}^e > \gamma^{1/4}\hat{\sigma}_{\rm n}^e$, it is recommended to use the corrected empirical estimator (35). It is the one that has the minimal bias and the minimal variance amongst all the estimators studied in this paper, but it can only be applied in the regime when the singular value corresponding to the target is outside the deformed quarter-circle distribution of the noise singular values.

• When $\hat{\sigma}_{\rm ref}^e < \gamma^{1/4}\hat{\sigma}_{\rm n}^e$, it is recommended to use the Kolmogorov–Smirnov estimator (37) with $K = 1$. Although its variance is larger than the one of the empirical estimator, its bias is much smaller and, as a result, it is the one that has the minimal quadratic error (sum of the squared bias and of the variance).

To summarize, the estimator of the noise variance that we will use in the following is

$$\hat{\sigma}_{\rm n}^f = \mathbf{1}_{\hat{\sigma}_{\rm ref}^e \le \gamma^{1/4}\hat{\sigma}_{\rm n}^e}\hat{\sigma}_{\rm n}^{K=1} + \mathbf{1}_{\hat{\sigma}_{\rm ref}^e > \gamma^{1/4}\hat{\sigma}_{\rm n}^e}\hat{\sigma}_{\rm n}^c. \tag{39}$$

Its bias and standard deviation are plotted in Figure 4.

6. Detection test

Consider the response matrix in the presence of measurement noise:

$$\boldsymbol{A}_{\rm meas} = \boldsymbol{A}_0 + \boldsymbol{W},$$

where $\boldsymbol{A}_0$ is zero in the absence of a target and equal to (4) when there is a target. The matrix $\boldsymbol{W}$ models additive measurement noise and its complex entries are independent and identically distributed with Gaussian statistics, mean zero and variance $\sigma_{\rm n}^2/M$.

The objective is to propose a detection test for the target. Since we know that the presence of a target is characterized by the existence of a significant singular

value, we propose to use a test of the form $R > r$ for the alarm corresponding to the presence of a target. Here R is the quantity obtained from the measured response matrix and defined by

$$R = \frac{\sigma_1^{(M)}}{\hat{\sigma}_{\mathrm{n}}}, \tag{40}$$

where $\hat{\sigma}_{\mathrm{n}}$ is the known value of σ_{n}, if known, or the estimator (39) of σ_{n}. Here the threshold value r of the test has to be chosen by the user. This choice follows from Neyman–Pearson theory as we explain below. It requires the knowledge of the statistical distribution of R which we give in the following proposition, which is a corollary of Proposition 4.2 (and Slutsky's theorem).

Proposition 6.1. *In the asymptotic regime $M \gg 1$ the following statements hold.*

(a) *In the absence of a target we have up to a term of order $o(M^{-2/3})$:*

$$R \simeq 1 + \gamma^{\frac{1}{2}} + \frac{1}{2M^{\frac{2}{3}}}(1+\gamma^{-\frac{1}{2}})^{\frac{1}{3}} Z_2, \tag{41}$$

where Z_2 follows a type-2 Tracy–Widom distribution.

(b) *In presence of a target*:

(b1) *If $\sigma_{\mathrm{ref}} > \gamma^{1/4}\sigma_{\mathrm{n}}$, then we have, up to a term of order $o(M^{-1/2})$,*

$$R \simeq \frac{\sigma_{\mathrm{ref}}}{\sigma_{\mathrm{n}}}\left(1+\gamma\frac{\sigma_{\mathrm{n}}^2}{\sigma_{\mathrm{ref}}^2}\right)^{\frac{1}{2}}\left(1+\frac{\sigma_{\mathrm{n}}^2}{\sigma_{\mathrm{ref}}^2}\right)^{\frac{1}{2}} + \frac{1}{2M^{\frac{1}{2}}}\left(\frac{\left(1-\gamma\sigma_{\mathrm{n}}^4/\sigma_{\mathrm{ref}}^4\right)\left(2+(1+\gamma)\sigma_{\mathrm{n}}^2/\sigma_{\mathrm{ref}}^2\right)}{\left(1+\gamma\sigma_{\mathrm{n}}^2/\sigma_{\mathrm{ref}}^2\right)\left(1+\sigma_{\mathrm{n}}^2/\sigma_{\mathrm{ref}}^2\right)^{\frac{1}{2}}}\right)^{\frac{1}{2}} Z_0, \tag{42}$$

where Z_0 follows a Gaussian distribution with mean zero and variance one.

(b2) *If $\sigma_{\mathrm{ref}} < \gamma^{1/4}\sigma_{\mathrm{n}}$, then we have* (41).

The data (i.e., the measured response matrix) gives the value of the ratio R. We propose to use a test of the form $R > r$ for the alarm corresponding to the presence of a target. The quality of this test can be quantified by two coefficients:

(1) The false alarm rate (FAR) is the probability to sound the alarm while there is no target:

$$\mathrm{FAR} = \mathbb{P}(R > r_\alpha | \text{ no target}).$$

(2) The probability of detection (POD) is the probability to sound the alarm when there is a target:

$$\mathrm{POD} = \mathbb{P}(R > r_\alpha | \text{ target}).$$

As is well-known in statistical test theory, it is not possible to find a test that minimizes the FAR and maximizes the POD. However, by the Neyman–Pearson lemma, the decision rule of sounding the alarm if and only if $R > r_\alpha$ maximizes the POD for a given FAR α, provided the threshold is taken to be equal to

$$r_\alpha = 1 + \gamma^{\frac{1}{2}} + \frac{1}{2M^{\frac{2}{3}}}(1+\gamma^{-\frac{1}{2}})^{\frac{1}{3}}\Phi_{\mathrm{TW2}}^{-1}(1-\alpha), \tag{43}$$

where Φ_{TW2} is the cumulative distribution function (19) of the Tracy–Widom distribution of type 2. The computation of the threshold r_α is easy since it depends only on the number of sensors N and M and on the FAR α. We have, for instance,

$$\Phi_{\mathrm{TW2}}^{-1}(0.9) \simeq -0.60, \quad \Phi_{\mathrm{TW2}}^{-1}(0.95) \simeq -0.23, \quad \Phi_{\mathrm{TW2}}^{-1}(0.99) \simeq 0.48.$$

These values are used in the detection tests whose POD are plotted in Figure 5.

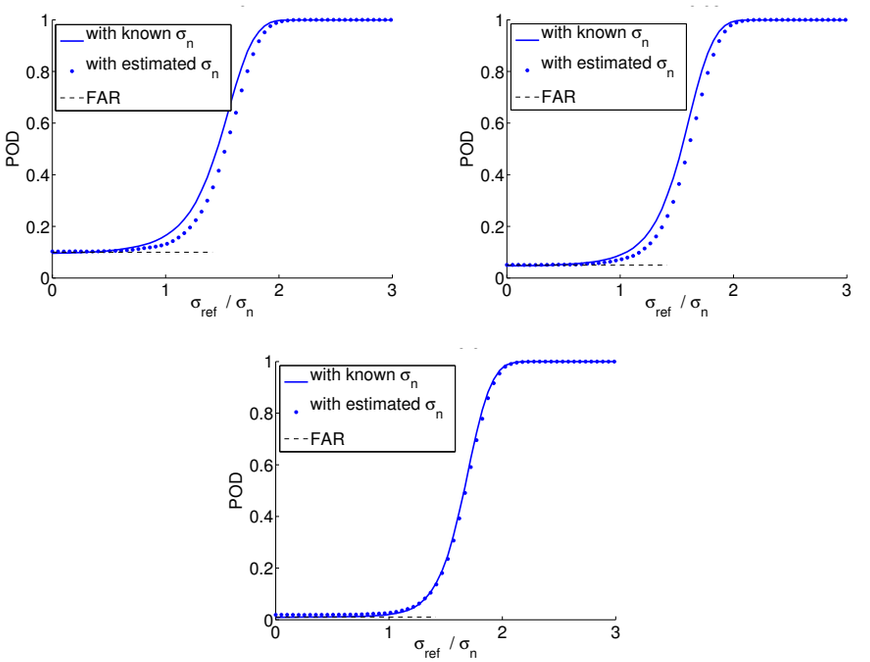

Figure 5. Probability of detection (POD) for the detection test calibrated with the threshold values r_α with $\alpha = 0.1$ (left), $\alpha = 0.05$ (right), and $\alpha = 0.01$ (bottom). Here $N = 200$ and $M = 50$. The blue solid and dotted lines correspond to the results of 10^4 MC simulations, in which the noise level is known (thick solid lines) or estimated by (39) (thick dotted lines). The dashed lines are the FAR desired in the absence of a target, which should be obtained when $\sigma_{\mathrm{ref}} = 0$.

The POD of this optimal test (optimal amongst all tests with the FAR α) depends on the value σ_{ref} and on the noise level σ_{n}. The theoretical test performance improves very rapidly with M when $\sigma_{\text{ref}} > \gamma^{1/4}\sigma_{\text{n}}$. When $\sigma_{\text{ref}} < \gamma^{1/4}\sigma_{\text{n}}$, so that the target is buried in noise (more exactly, the singular value corresponding to the target is buried in the deformed quarter-circle distribution of the other singular values), then we have $\text{POD} = 1 - \Phi_{\text{TW2}}(\Phi_{\text{TW2}}^{-1}(1-\alpha)) = \alpha$.

The POD of the test (40) calibrated for different values of the FAR is plotted in Figure 5. One can observe that the calibration with r_α gives the desired FAR and that the POD rapidly goes to one when the singular value σ_{ref} of the target becomes larger than $\gamma^{1/4}\sigma_{\text{n}}$. Furthermore, the use of the estimator (39) for the noise level σ_{n} is also very efficient in that we get almost the same FAR and POD with the true value σ_{n} as with the estimator $\hat{\sigma}_{\text{n}}^{f}$. In Figure 6 we plot the POD obtained with other estimators of the noise level in order to confirm that the estimator $\hat{\sigma}_{\text{n}}^{f}$ defined by (39) is indeed the most appropriate.

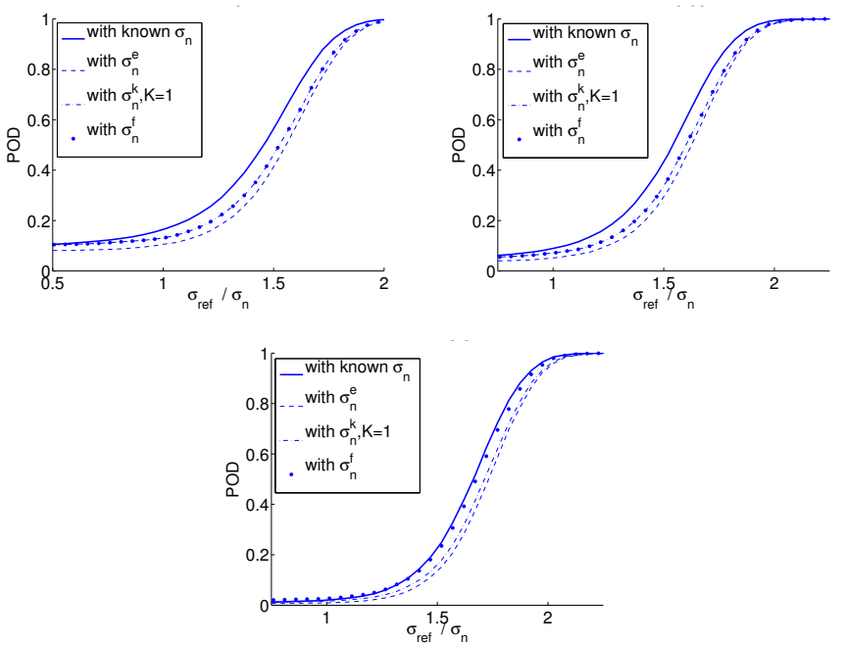

Figure 6. Probability of detection (POD) for the detection test calibrated with the threshold values r_α with $\alpha = 0.1$ (left), $\alpha = 0.05$ (right), and $\alpha = 0.01$ (bottom). Here $N = 200$ and $M = 50$. The blue lines correspond to the results of 10^4 MC simulations, in which the noise level is known (thick solid lines) or estimated by (39) (thick dotted lines) or estimated by the estimators (30) and (37) (thin dashed lines).

7. Target localization and reconstruction

In this section we would like to present simple and robust way to localize the target and reconstruct its properties once the detection test has passed. By simple we mean that we will only use the first singular value and left singular vector of the response matrix, and by robust we mean a procedure that allows for estimations with bias and variance as small as possible.

Localization. A standard imaging functional is the MUSIC functional defined by [Ammari et al. 2011]:

$$\mathcal{I}_{\mathrm{MUSIC}}(\boldsymbol{x}) := \big\| \boldsymbol{u}(\boldsymbol{x}) - \big(\boldsymbol{u}_1^{(M)^\dagger} \boldsymbol{u}(\boldsymbol{x})\big)\boldsymbol{u}_1^{(M)} \big\|^{-\frac{1}{2}} = \big(1 - \big|\boldsymbol{u}(\boldsymbol{x})^\dagger \boldsymbol{u}_1^{(M)}\big|^2\big)^{-\frac{1}{2}},$$

where $\boldsymbol{u}(\boldsymbol{x})$ is the normalized vector of Green's functions (8) and $\boldsymbol{u}_1^{(M)}$ is the first left singular vector of the measured response matrix $\boldsymbol{A}_{\mathrm{meas}}$. The MUSIC functional is the projection of the Green's vector $\boldsymbol{u}(\boldsymbol{x})$ from the receiver array to the search point $\boldsymbol{x}$ onto the noise space of the measured response matrix.

In the absence of noise the MUSIC functional presents a peak at $\boldsymbol{x} = \boldsymbol{x}_{\mathrm{ref}}$. Indeed, in this case, we have $\boldsymbol{u}_1^{(M)} = \boldsymbol{u}(\boldsymbol{x}_{\mathrm{ref}})$ (up to a phase term) and therefore $\mathcal{I}_{\mathrm{MUSIC}}(\boldsymbol{x})$ becomes singular at $\boldsymbol{x} = \boldsymbol{x}_{\mathrm{ref}}$. Furthermore, we can quantify the accuracy of the reflector localization as follows. When the arrays surround the search region, the singular vectors $\boldsymbol{u}(\boldsymbol{x})$ can be shown to be orthogonal to $\boldsymbol{u}(\boldsymbol{x}_{\mathrm{ref}})$ when the distance between the search point $\boldsymbol{x}$ and the target point $\boldsymbol{x}_{\mathrm{ref}}$ becomes larger than half a wavelength. This can be shown using Helmholtz–Kirchhoff identity and this gives the resolution of the imaging functional: one can get the position of the reflector within the accuracy of half a wavelength. When the arrays are partial, then the accuracy can be described in terms of the so-called Rayleigh resolution formulas [Elmore and Heald 1969; Garnier and Papanicolaou 2010].

In the presence of noise the peak of the MUSIC functional is affected. By Proposition 4.3, in the regime $M \gg 1$, the value of the MUSIC functional at an arbitrary point $\boldsymbol{x} \neq \boldsymbol{x}_{\mathrm{ref}}$ is one while the theoretical value at $\boldsymbol{x} = \boldsymbol{x}_{\mathrm{ref}}$ is given by

$$\mathcal{I}_{\mathrm{MUSIC}}(\boldsymbol{x}_{\mathrm{ref}}) = (1 - c_u)^{-\frac{1}{2}},$$

where c_u is the theoretical angle between the first left singular vector $\boldsymbol{u}(\boldsymbol{x}_{\mathrm{ref}})$ of the unperturbed matrix $\boldsymbol{A}_0$ and the first left singular vector $\boldsymbol{u}_1^{(M)}$ of the measured response matrix $\boldsymbol{A}_{\mathrm{meas}}$:

$$c_u = \begin{cases} \dfrac{1 - \gamma\sigma_{\mathrm{n}}^4/\sigma_{\mathrm{ref}}^4}{1 + \gamma\sigma_{\mathrm{n}}^2/\sigma_{\mathrm{ref}}^2} & \text{if } \sigma_{\mathrm{ref}} > \gamma^{\frac{1}{4}}\sigma_{\mathrm{n}}, \\ 0 & \text{if } \sigma_{\mathrm{ref}} < \gamma^{\frac{1}{4}}\sigma_{\mathrm{n}}. \end{cases}$$

Therefore, provided the detection test has passed, which means that the target singular value is larger than the noise singular values, the MUSIC algorithm gives a robust and simple way to estimate the position of the reflector. The estimator of $\boldsymbol{x}_{\mathrm{ref}}$ that we propose is

$$\hat{\boldsymbol{x}}_{\mathrm{ref}} := \operatorname*{argmax}_{\boldsymbol{x}} \mathcal{I}_{\mathrm{MUSIC}}(\boldsymbol{x}). \tag{44}$$

Note that more complex and computationally expensive algorithms (using reverse-time migration) can improve the quality of the estimation as shown in [Ammari et al. 2012].

Reconstruction. Using Proposition 4.2 we can see that the quantity

$$\hat{\sigma}_{\mathrm{ref}} = \frac{\hat{\sigma}_{\mathrm{n}}}{\sqrt{2}} \left\{ \left(\frac{\sigma_1^{(M)}}{\hat{\sigma}_{\mathrm{n}}} \right)^2 - 1 - \gamma + \left(\left[\left(\frac{\sigma_1^{(M)}}{\hat{\sigma}_{\mathrm{n}}} \right)^2 - 1 - \gamma \right]^2 - 4\gamma \right)^{\frac{1}{2}} \right\}^{\frac{1}{2}} \tag{45}$$

is an estimator of σ_{ref}, provided that $\sigma_{\mathrm{ref}} > \gamma^{\frac{1}{4}} \sigma_{\mathrm{n}}$. Here $\hat{\sigma}_{\mathrm{n}}$ is the known value of σ_{n}, if known, or the estimator (39) of σ_{n}. In practice, if the detection test passes, then this implies that we are in this case. From (6) we can therefore estimate the scattering amplitude ρ_{ref} of the inclusion by

$$\hat{\rho}_{\mathrm{ref}} = \frac{c_0^2}{\omega^2} \left(\sum_{n=1}^{N} |\hat{G}(\omega, \hat{\boldsymbol{x}}_{\mathrm{ref}}, \boldsymbol{y}_n)|^2 \right)^{-\frac{1}{2}} \left(\sum_{m=1}^{M} |\hat{G}(\omega, \hat{\boldsymbol{x}}_{\mathrm{ref}}, \boldsymbol{z}_m)|^2 \right)^{-\frac{1}{2}} \hat{\sigma}_{\mathrm{ref}}, \tag{46}$$

with $\hat{\sigma}_{\mathrm{ref}}$ the estimator (45) of σ_{ref} and $\hat{\boldsymbol{x}}_{\mathrm{ref}}$ is the estimator (44) of the position of the inclusion. This estimator is not biased asymptotically because it compensates for the level repulsion of the first singular value due to the noise.

Numerical simulations. We consider the following numerical set-up: the wavelength is equal to one. There is one reflector with scattering amplitude $\rho_{\mathrm{ref}} = 1$, located at $\boldsymbol{x}_{\mathrm{ref}} = (0, 0, 50)$. We consider a linear array of $N = 200$ transducers located half a wavelength apart on the line from $(-50, 0, 0)$ to $(50, 0, 0)$. Each transducer is used as a receiver, but only one of four is used as a source (therefore, $M = 50$ and $\gamma = 4$). The noise level is $\sigma_{\mathrm{n}} = \sigma_{\mathrm{ref}}/4$ or $\sigma_{\mathrm{ref}}/2$, where σ_{ref} is the singular value associated to the reflector (given by (6)).

We have carried out a series of 10^4 MC simulations (using the estimator (39) of σ_{n}). The results are reported in Figure 7 for $\sigma_{\mathrm{n}} = \sigma_{\mathrm{ref}}/4$ and in Figure 8 for $\sigma_{\mathrm{n}} = \sigma_{\mathrm{ref}}/2$:

(1) The reflector is always detected when $\sigma_{\mathrm{n}} = \sigma_{\mathrm{ref}}/4$ and it is detected with probability 97% when $\sigma_{\mathrm{n}} = \sigma_{\mathrm{ref}}/2$ (in agreement with the POD plotted in

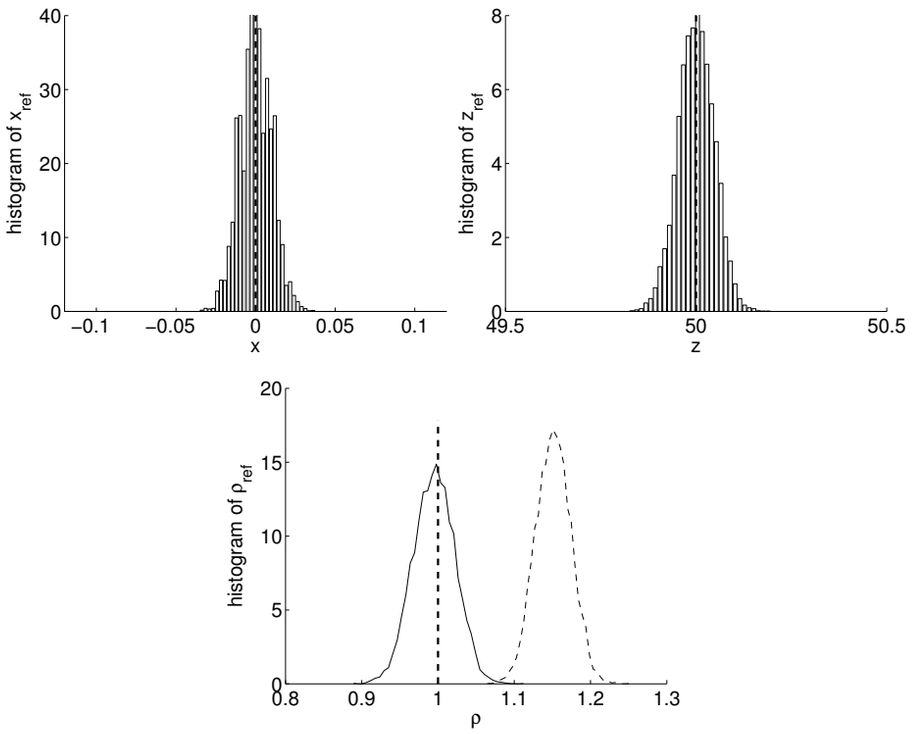

Figure 7. Top: histograms of the estimated cross-range position $\hat{x}_{\rm ref}$ (left) and estimated range position $\hat{z}_{\rm ref}$ (right) given by (44). Bottom: histogram of the estimated scattering amplitude $\hat{\rho}_{\rm ref}$ given by (46) (solid lines) or $\hat{\rho}^e_{\rm ref}$ given by (47) (dashed lines). Here $\sigma_{\rm n} = \sigma_{\rm ref}/4$.

Figure 5).

(2) The estimator $\hat{\boldsymbol{x}}_{\rm ref}$ defined by (44) of the position of the reflector has good properties. The histograms of the estimated positions $\hat{\boldsymbol{x}}_{\rm ref} = (\hat{x}_{\rm ref}, 0, \hat{z}_{\rm ref})$ are plotted in the top row of Figures 7 and 8.

(3) The estimator $\hat{\rho}_{\rm ref}$ defined by (46) of the scattering amplitude has no bias because it uses the inversion formula (45) which compensates for the level repulsion of the first singular value. We plot in the bottom row of Figures 7 and 8 the histogram of the estimated scattering amplitude and we compare with the empirical estimator

$$\hat{\rho}^e_{\rm ref} = \frac{c_0^2}{\omega^2}\left(\sum_{n=1}^{N} |\hat{G}(\omega, \hat{\boldsymbol{x}}_{\rm ref}, \boldsymbol{y}_n)|^2\right)^{-\frac{1}{2}} \left(\sum_{m=1}^{M} |\hat{G}(\omega, \hat{\boldsymbol{x}}_{\rm ref}, \boldsymbol{z}_m)|^2\right)^{-\frac{1}{2}} \sigma_1^{(M)}, \tag{47}$$

which has a large bias.

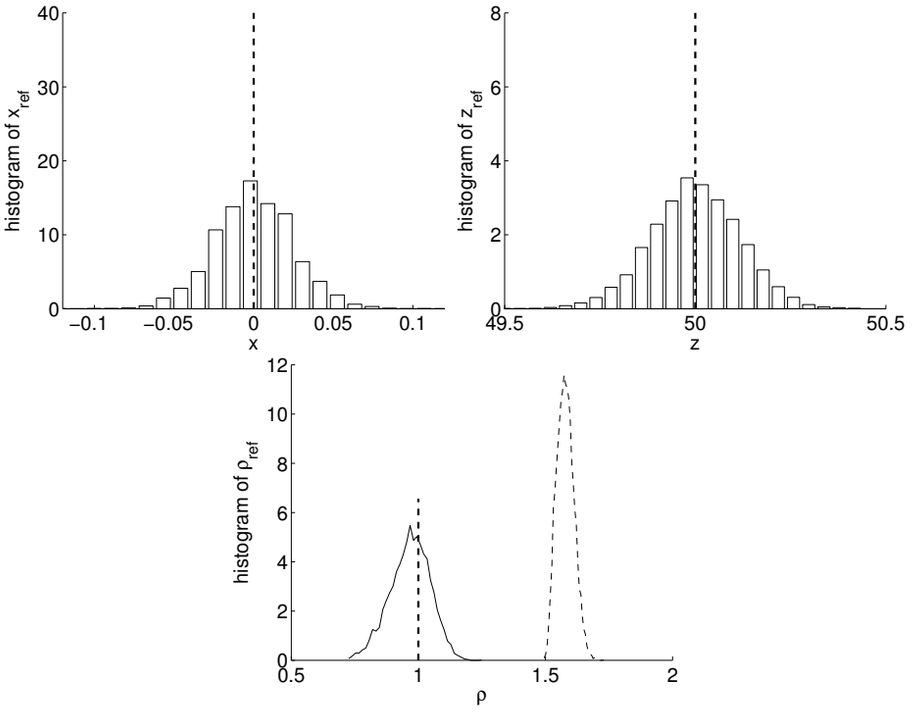

Figure 8. The same as in Figure 7, but here $\sigma_{\mathrm{n}} = \sigma_{\mathrm{ref}}/2$.

8. Conclusion

In this paper we have presented a few results that show how random matrix theory can be used in sensor array imaging. It turns out that most of the needed results are already available in the literature in the case addressed in this paper, that is, when the response matrix is perturbed by an additive measurement noise. However, the most interesting questions arise in the presence of clutter noise, which is the case in which the data are corrupted by perturbations due to random heterogeneities present in the medium. In this case the random perturbation of the response matrix cannot be described in terms of an additive uncorrelated noise, but it has special correlation structure [Aubry and Derode 2009a; Fouque et al. 2007]. This case certainly deserves more attention and more work.

References

[Ammari and Kang 2004] H. Ammari and H. Kang, *Reconstruction of small inhomogeneities from boundary measurements*, Lecture Notes in Mathematics **1846**, Springer, Berlin, 2004.

[Ammari and Volkov 2005] H. Ammari and D. Volkov, "The leading-order term in the asymptotic expansion of the scattering amplitude of a collection of finite number of dielectric inhomogeneities

of small diameter", *International Journal for Multiscale Computational Engineering* **3** (2005), 149–160.

[Ammari et al. 2001] H. Ammari, M. S. Vogelius, and D. Volkov, "Asymptotic formulas for perturbations in the electromagnetic fields due to the presence of inhomogeneities of small diameter, II: The full Maxwell equations", *J. Math. Pures Appl.* (9) **80**:8 (2001), 769–814.

[Ammari et al. 2011] H. Ammari, J. Garnier, H. Kang, W.-K. Park, and K. Sølna, "Imaging schemes for perfectly conducting cracks", *SIAM J. Appl. Math.* **71**:1 (2011), 68–91.

[Ammari et al. 2012] H. Ammari, J. Garnier, and K. Sølna, "A statistical approach to target detection and localization in the presence of noise", *Waves Random Complex Media* **22**:1 (2012), 40–65.

[Angelsen 2000] B. Angelsen, *Ultrasound imaging: waves, signals and signal processing*, Emantec, Trondheim, 2000.

[Aubry and Derode 2009a] A. Aubry and A. Derode, "Detection and imaging in a random medium: A matrix method to overcome multiple scattering and aberration", *J. Appl. Physics* **106** (2009), 044903.

[Aubry and Derode 2009b] A. Aubry and A. Derode, "Random matrix theory applied to acoustic backscattering and imaging in complex media", *Phys. Rev. Lett.* **102** (2009), 084301.

[Aubry and Derode 2010] A. Aubry and A. Derode, "Singular value distribution of the propagation matrix in random scattering media", *Waves in Random and Complex Media* **20**:3 (2010), 333–363.

[Baik et al. 2005] J. Baik, G. Ben Arous, and S. Péché, "Phase transition of the largest eigenvalue for nonnull complex sample covariance matrices", *Ann. Probab.* **33**:5 (2005), 1643–1697.

[Baik et al. 2008] J. Baik, R. Buckingham, and J. DiFranco, "Asymptotics of Tracy–Widom distributions and the total integral of a Painlevé II function", *Comm. Math. Phys.* **280**:2 (2008), 463–497.

[Benaych-Georges and Nadakuditi 2011] F. Benaych-Georges and R. R. Nadakuditi, "The eigenvalues and eigenvectors of finite, low rank perturbations of large random matrices", *Adv. Math.* **227**:1 (2011), 494–521.

[Bornemann 2010] F. Bornemann, "On the numerical evaluation of distributions in random matrix theory: a review", *Markov Process. Related Fields* **16**:4 (2010), 803–866.

[Capitaine et al. 2012] M. Capitaine, C. Donati-Martin, and D. Féral, "Central limit theorems for eigenvalues of deformations of Wigner matrices", *Ann. Inst. Henri Poincaré Probab. Stat.* **48**:1 (2012), 107–133.

[Chapon et al. 2014] F. Chapon, R. Couillet, W. Hachem, and X. Mestre, "The outliers among the singular values of large rectangular random matrices with additive fixed rank deformation", *Markov Processes and Related Fields* (2014). Accepted for publication. arXiv 1207.0471

[Elmore and Heald 1969] W. Elmore and M. Heald, *Physics of waves*, Dover, New York, 1969.

[Fouque et al. 2007] J.-P. Fouque, J. Garnier, G. Papanicolaou, and K. Sølna, *Wave propagation and time reversal in randomly layered media*, Stochastic Modelling and Applied Probability **56**, Springer, New York, 2007.

[Garnier and Papanicolaou 2010] J. Garnier and G. Papanicolaou, "Resolution analysis for imaging with noise", *Inverse Problems* **26**:7 (2010), 074001, 22.

[Györfi et al. 1996] L. Györfi, I. Vajda, and E. van der Meulen, "Minimum Kolmogorov distance estimates of parameters and parametrized distributions", *Metrika* **43**:3 (1996), 237–255.

[Hadamard 1893] J. Hadamard, "Résolution d'une question relative aux déterminants", *Bull. Sci. Math.* **17** (1893), 30–31.

[Johnstone 2001] I. M. Johnstone, "On the distribution of the largest eigenvalue in principal components analysis", *Ann. Statist.* **29**:2 (2001), 295–327.

[Marchenko and Pastur 1967] V. A. Marchenko and L. A. Pastur, "Distribution of eigenvalues in some sets of random matrices", *Mat. Sb.* (*N.S.*) **72 (114)** (1967), 507–536. In Russian. Translated in *Math. USSR Sbornik* **1** (1967), 457–483.

[Shabalin and Nobel 2013] A. A. Shabalin and A. B. Nobel, "Reconstruction of a low-rank matrix in the presence of Gaussian noise", *J. Multivariate Anal.* **118** (2013), 67–76.

[Stergiopoulos 2001] S. Stergiopoulos, *Advanced signal processing handbook: theory and implementation for radar, sonar, and medical imaging real-time systems*, CRC Press, Boca Raton, FL, 2001.

Laboratoire de Probabilités et Modèles Aléatoires & Laboratoire Jacques-Louis Lions, Université Paris VII, 75205 Paris Cedex 13, France
garnier@math.univ-paris-diderot.fr

Department of Mathematics, University of California, Irvine, CA 92697, United States
ksolna@math.uci.edu